Persistence and Eventual Demise of Oxygen Molecules at Terapascal Pressures

Jian Sun,[1,*] Miguel Martinez-Canales,[2] Dennis D. Klug,[3] Chris J. Pickard,[2] and Richard J. Needs[4]

[1]*Lehrstuhl für Theoretische Chemie, Ruhr-Universität Bochum, 44780 Bochum, Germany*
[2]*Department of Physics and Astronomy, University College London, Gower Street, London WC1E 6BT, United Kingdom*
[3]*Steacie Institute for Molecular Sciences, National Research Council of Canada, Ottawa, K1A 0R6, Canada*
[4]*Theory of Condensed Matter Group, Cavendish Laboratory, J J Thomson Avenue, Cambridge CB3 0HE, United Kingdom*

(Received 7 November 2011; published 27 January 2012)

Computational searches for structures of solid oxygen under high pressures in the multi-TPa range are carried out using density-functional-theory methods. We find that molecular oxygen persists to about 1.9 TPa at which it transforms into a semiconducting square-spiral-like polymeric structure ($I4_1/acd$) with a band gap of ~3.0 eV. Solid oxygen forms a metallic zigzag chainlike structure ($Cmcm$) at about 3.0 TPa, but the chains in each layer gradually merge as the pressure is increased and a structure of $Fmmm$ symmetry forms at about 9.3 TPa in which each atom has four nearest neighbors. The superconducting properties of molecular oxygen do not vary much with compression, although the structure becomes more symmetric. The electronic properties of oxygen have a complex evolution with pressure, swapping between insulating, semiconducting, and metallic.

DOI: 10.1103/PhysRevLett.108.045503 PACS numbers: 61.50.Ks, 71.20.−b, 81.05.Zx, 81.40.Vw

Among the simple molecules studied at high pressures, oxygen has attracted particular attention due to its fundamental importance and intriguing properties. [1–5] For example, oxygen is the only known elemental molecular solid that exhibits magnetism, which adds substantial complexity to its phase diagram. When liquid oxygen is cooled at ambient pressure it undergoes a sequence of transitions to the γ, β and α solid phases at 54.39, 43.76, and 23.88 K, respectively [6]. Upon increase of pressure the monoclinic α-O_2 ($C2/m$) phase transforms into an orthorhombic δ-O_2 ($Fmmm$) phase at about 3 GPa and to ϵ-O_2 at about 10 GPa. The structure of ϵ-O_2 has only recently been solved by x-ray diffraction (XRD) studies of single crystal [3] and powder [4] samples, although its vibrational spectrum was reported more than 20 years earlier [7]. The unit cell of ϵ-O_2 has $C2/m$ symmetry and contains four O_2 molecules forming O_8 units. Both α and δ-O_2 are antiferromagnetic and the magnetic collapse at the δ-ϵ transition was predicted using molecular dynamics simulations [8]. This breakdown of the long-range antiferromagnetic order at about 8 GPa was recently observed in a neutron scattering experiment [2]. Density-functional-theory (DFT) studies have found another chainlike structure to be energetically slightly more favorable than the O_8 structure [9,10], although it has not been observed in experiments.

Recent experiments [5] have shown that insulating ϵ-O_2 remains stable up to about 96 GPa before undergoing a continuous displacive and isosymmetric transition to the ζ phase, in agreement with earlier predictions [10]. The metallic ζ phase [11,12] has $C2/m$ symmetry [2] and superconducts at temperatures below 0.6 K [1]. Many-body perturbation theory GW calculations [13,14] have suggested that the metal-insulator transition occurs at lower pressures than the measured ϵ-ζ transition pressure of 96 GPa. The above information, however, covers only a small part of the phase diagram and rather little is known about pure oxygen at pressures above 100 GPa.

A previous DFT study reported that oxygen molecules persist to at least 250 GPa [10]. It is interesting to speculate about the highest pressure to which oxygen molecules can survive, and whether oxygen forms polymeric materials as found in N_2 [15–17], CO [18,19], and CO_2 [20,21], and predicted in H_2 [22,23]. Materials under terapascal pressures are of great interest in planetary science, for example, the pressure at the center of Jupiter is estimated to be about 7 TPa [24]. Recent progress in dynamical shock wave [24–26] and ramped compression experiments [27,28] has demonstrated that the terapascal pressure regime is becoming much more accessible.

The use of DFT computations combined with searching methods has provided a new route for predicting the structures and energetics of high-pressure phases [23,29,30]. A very recent study of phase transitions, melting, and chemical reactivity in CO_2 found it to dissociate into carbon and oxygen above 33 GPa and 1720 K [31], which adds further motivation for studying pure oxygen at high pressures. In this work we focus on oxygen at ultrahigh pressures up to the terapascal regime, finding very surprising behavior.

We have used the *ab initio* random structure searching (AIRSS) method [32,33] and DFT calculations to identify low-enthalpy structures of oxygen in the multi-TPa range. We used the Perdew-Burke-Ernzerhof (PBE) [34] generalized gradient approximation (GGA) exchange-correlation density functional. The searches were performed using the CASTEP plane-wave DFT code [35] and ultrasoft pseudopotentials. Searches were performed at selected combinations of 0.5, 1, 2, 3, 4, 5, and 8 TPa, with 6, 8, 9, 10, 12, and

16 oxygen atoms per cell. A total of about 14 000 relaxed structures were generated in the searches. The enthalpy-pressure relations were then recalculated using very hard projector augmented wave (PAW) pseudopotentials and the VASP code [36] with a plane-wave basis set cutoff energy of 900 eV. Phonon and electron-phonon coupling calculations were performed using DFT perturbation theory and the ABINIT code [37], norm-conserving pseudopotentials, the PBE functional, and an energy cutoff of 1632 eV. Further details of the calculations are given in the supplementary material [38].

The enthalpy-pressure relations for the most interesting structures are plotted in Fig. 1. We predict that at about 1.9 TPa molecular oxygen should transform into a square-spiral-like structure belonging to space group $I4_1/acd$, as shown in the inset in the lower left corner of Fig. 1. Similar structures have been found in other heavier group VI elements, such as sulfur and selenium [39]. The shortest O-O bond length in $I4_1/acd$ at 2 TPa is about 1.15 Å, which is longer than that of the molecular phase at the same pressure (about 1.03 Å). The shortest O-O distance between the chains is about 1.55 Å, and the distance between the axes of neighboring square spirals is half of the lattice vector. The O-O-O angle in the helix is about 98.7°.

At about 3.0 TPa, the square-spiral phase transforms into a zigzag chainlike phase of *Cmcm* symmetry, as shown in Fig. 1. The O-O bond length within the chains is 1.10 Å at 3.5 TPa, while the interchain O-O separation in the plane is 1.33 Å. The O-O-O angle within the chain is 102.8°. With increasing pressure the chains in each layer of *Cmcm* gradually merge and at about 9.3 TPa a structure of

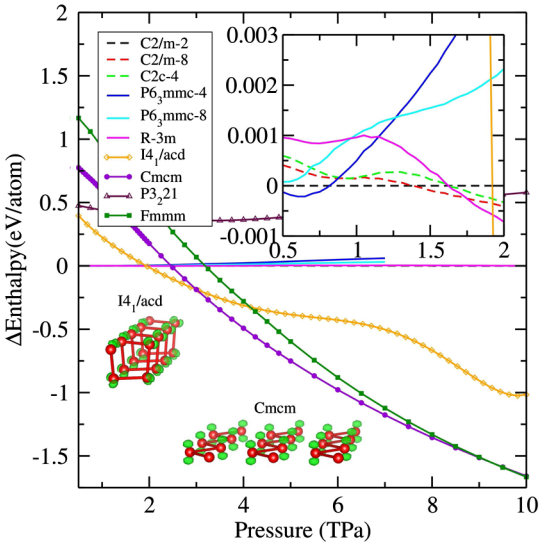

FIG. 1 (color online). Enthalpy-pressure relations for solid oxygen. The upper right inset shows the enthalpies of the molecular phases, while the insets in the lower left corner show the square-spiral structure of $I4_1/acd$ and zigzag chains of *Cmcm*, respectively. The green bubbles represent the electron lone pairs.

Fmmm symmetry forms in which each atom has four nearest neighbors at a separation of 1.05 Å.

The low-pressure molecular phases are very close in enthalpy, as the inset of Fig. 1 shows. Among these phases, $P6_3/mmc$-4, $C2/m$-2, $C2/m$-8, and $R\bar{3}m$ become stable in turn on increasing the pressure from 0.5 to 1.9 TPa. More precise methods than DFT might be required to clarify the structural sequence as the enthalpy differences are so small. Although the O = O bond in the O_2 molecule is not as strong as the N ≡ N and C ≡ O triple bonds, O_2 polymerizes at a much higher pressure than N_2 (~ 110 GPa [15]) and CO (experiments show that CO polymerizes at about 5 GPa [18] while calculations predict that it could even polymerize at ambient pressure [19]). The fact that the molecular phases persist to pressures as high as 1.9 TPa is intriguing. Electron counting arguments indicate that an oxygen atom can form two covalent bonds, either a double bond as in the O_2 molecule or two single bonds, as would be expected in polymerized oxygen. The double bonds of the molecule are shorter and stronger than the single bonds of polymerized forms, and the lone electron pairs on the oxygen atoms result in bent bonds, as in the ozone O_3 molecule, and give rise to strongly repulsive interactions between the molecules and between the polymeric chains. The great reluctance of oxygen to form more than two covalent bonds, the requirement that these bonds be bent, and the lone-pair repulsion greatly limits the forms of dense structures which may occur. The square spirals of the $I4_1/acd$ structure are not well packed and, while the zigzag chains of *Cmcm* pack more efficiently, there is no bonding between chains so that very dense structures are not formed. These factors lead to the persistence of molecular forms to high pressures, and the absence of stable framework structures up to at least 10 TPa.

We studied other possible candidate structural types such as buckled octagons of the type found in the S-I phase of sulfur ($Fddd$) and the threefold spiral-like $P3_221$ structure of S-II [39], but these were found to be much less stable than the best structures obtained in our searches. The transition pressures between the most favorable phases were recalculated using several different exchange-correlation functionals, but the results were found to be insensitive to the choice of functional [38].

The electronic band structures and projected electronic densities of states (PDoS) of $R\bar{3}m$ at 1.8 TPa, $I4_1/acd$ at 2.0 TPa and *Cmcm* at 3.5 TPa are shown in Fig. 2, decomposed into *s* and *p* components. As mentioned above, the enthalpies of the molecular phases are very close, but the $R\bar{3}m$ structure is the most likely molecular ground state prior to polymerization at 1.9 TPa. Our DFT calculations suggest that the $R\bar{3}m$ structure is metallic at 1.8 TPa and the electronic density of states at the Fermi level mostly derives from the *p* electrons.

Surprisingly, it turns out that the square-spiral-like $I4_1/acd$ phase has a band gap of 3.0 eV at 2.0 TPa, as

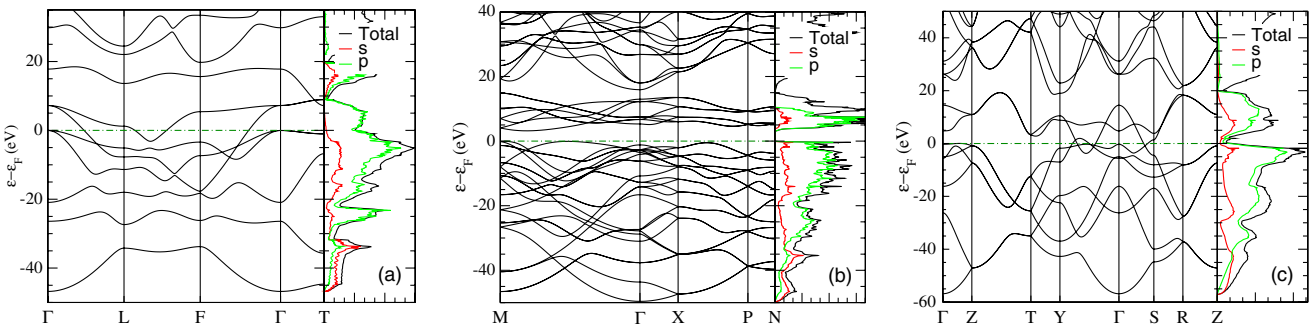

FIG. 2 (color online). Electronic band structures and projected densities of states (PDoS). (a) $R\bar{3}m$ at 1.8 TPa, (b) $I4_1/acd$ at 2.0 TPa, and (c) $Cmcm$ at 3.5 TPa. The zero of energy is at the Fermi level.

shown in Fig. 2(b). Considering that standard density functionals such as PBE are well-known for underestimating band gaps, $I4_1/acd$ is expected to be a wide-gap semiconductor. As shown in the electron density plots of Figs. 3(a) and 3(b), and also in the charge density difference in the lower left inset of Fig. 1, the electrons are strongly localized. Strong covalent bonds are formed along the spiral chains and the projections of the electron density on the [100] and [001] planes show that the spirals are separated and not bonded to each other.

The calculated PDoS and band gap of the $Cmcm$ phase [Fig. 2(c)] show that oxygen is metallic at 3.5 TPa. The density of states at the Fermi level derives approximately equally from the s and p electrons and is smaller than that of the $R\bar{3}m$ structure [Fig. 2(a)]. This indicates that the $Cmcm$ phase is a weak metal and supports the conclusion that the lone-pair electrons are not very extended. The electron density plots of Figs. 3(c) and 3(d) show that the zigzag chains are not bonded to one another and that the layers are well separated.

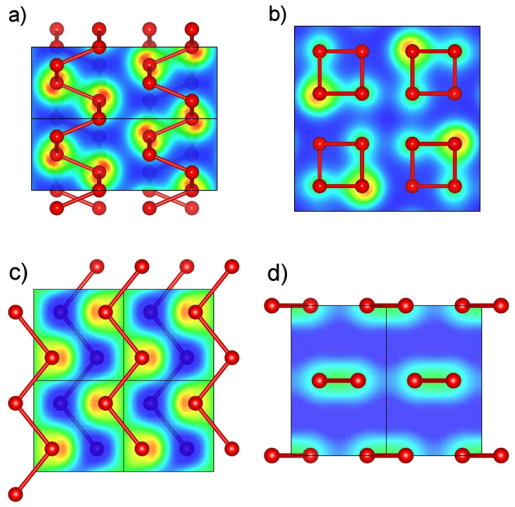

FIG. 3 (color online). Electronic densities of polymeric oxygen. (a) and (b) $I4_1/acd$ at 2.0 TPa along the [100] and [001] directions, (c) and (d) $Cmcm$ at 3.5 TPa along the [100] and [001] directions.

We calculated phonon dispersion relations of the high-pressure phases that we predict to have regions of thermodynamic stability. We found that $C2/m$-2 is dynamically stable at 1 TPa, $R\bar{3}m$ is stable at 1.0 and 1.8 TPa, $I4_1/acd$ is stable at 2.0 TPa, $Cmcm$ is stable at 3.5 and 3.8 TPa, and that $Fmmm$ is stable at 11 TPa, see Fig. 4 and supplementary materials [38]. The dynamical stability of the $R\bar{3}m$, $I4_1/acd$ and $Cmcm$ structures was confirmed with both the PBE and local density approximation (LDA) functionals [38]. Structure $C2/m$-2 and $R\bar{3}m$ have a group-subgroup relation which may indicate that oxygen molecules symmetrize upon increasing pressure near the transformation to polymeric phases. The molecular ζ oxygen is a superconductor at temperatures below 0.6 K [1]. We have therefore calculated the phonon linewidth, Eliashberg function $\alpha^2F(\omega)$, electron-phonon coupling (EPC) constant λ, and the logarithmic average phonon frequency $\omega_{\log}$, to investigate whether the molecular $R\bar{3}m$ and polymeric $Cmcm$ phases of oxygen are superconducting.

As shown in Fig. 4 (upper), the acoustic phonon modes and the intramolecular LO modes of $R\bar{3}m$ have relatively large linewidths close to the Γ point, while the TO modes have large linewidths along L-F. We have used the Allen-Dynes modification of the McMillan equation for the superconducting transition temperature [40], $T_c = \omega_{\log}/1.2\exp[-1.04(1+\lambda)/\lambda - \mu^*(1+0.62\lambda)]$, where μ^* is the Coulomb pseudopotential, with typical values of μ^* between 0.10 and 0.13. The calculated isotropic EPC constant for the $R\bar{3}m$ structure at 1.8 TPa is about 0.34 and T_c varies from 2.1 to 0.6 K, which is close to the value observed for the ζ phase of about 0.6 K [1].

The phonon band structure of $I4_1/acd$ at 2.0 TPa is shown in Fig. 4 (lower left). The phonon dispersion along X-P and P-N is small, indicating that the bonding between the square spirals is weak. The phonon dispersion relation of $Cmcm$ at 3.5 TPa (Fig. 4 lower right) shows the structure to be stable and highly anisotropic. Chain-like and layered structures also appear in other molecular systems, such as CO [19,21] and N_2 [17].

We have investigated oxygen under terapascal pressures using the AIRSS technique and *ab initio* DFT calculations.

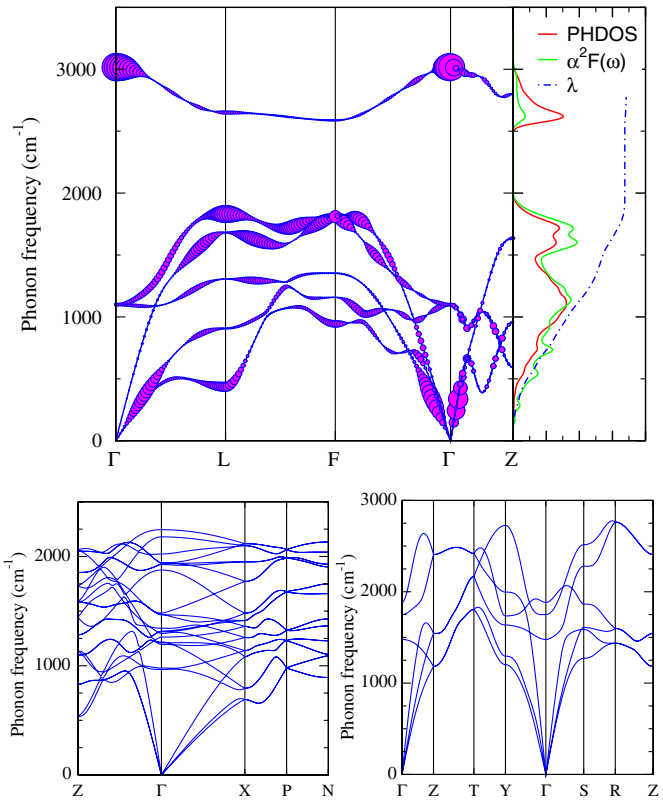

FIG. 4 (color online). Phonon dispersion relations of $R\bar{3}m$ at 1.8 TPa (upper), $I4_1/acd$ at 2.0 TPa (lower left) and $Cmcm$ at 3.5 TPa (lower right). The blue circles with magenta filling show the phonon linewidth at different wave vectors.

Oxygen molecules persist up to about 1.9 TPa, which is almost 1 order of magnitude larger than previously reported [10] and also much larger than other diatomic molecules such as H_2, N_2, and CO. Oxygen polymerizes at about 1.9 TPa giving a square-spiral-like structure of space group $I4_1/acd$, which is a semiconductor with a DFT band gap of about 3.0 eV. The $R\bar{3}m$ structure is superconducting at 1.8 TPa and has a similar T_c to the ζ phase. The metallic $R\bar{3}m$ is slightly more stable than other molecular forms at high pressures and the oxygen molecules symmetrize before polymerization. Temperature might have a significant effect on the transition from molecular to polymeric oxygen phases, as found in CO_2 [21], but more detailed simulations would be required to address this point. At about 3.0 TPa, the system collapses to a denser metallic $Cmcm$ phase, which consists of zigzag chains. The stability of molecular and chainlike phases of highly-compressed solid oxygen demonstrates that the electron counting rule is effective up to multi-TPa pressures. Merging of the chains in each layer of $Cmcm$ leads to the formation of a phase of $Fmmm$ symmetry at 9.3 TPa in which each atom has four nearest neighbors, which signals the eventual failure of the electron counting rule to predict the bonding. The strongly repulsive interactions between the lone pairs hinders the polymerization of the molecules and the formation of more highly coordinated structures. The electronic structure of oxygen changes dramatically with increasing pressure. It transforms from the insulating ϵ phase to the molecular metal ζ phase, which persists up to 1.9 TPa, where it transforms into the semiconducting $I4_1/acd$ polymeric phase, eventually returning to metallic behavior with the appearance of the $Cmcm$ phase at about 3.0 TPa.

J. S. gratefully acknowledges financial support from the Alexander von Humboldt (AvH) foundation. C. J. P. and R. J. N. were supported by the EPSRC. The calculations were carried out at BOVILAB@RUB (Bochum), on the supercomputers at NRC (Ottawa) and UCL.

*jian.sun@theochem.rub.de

[1] K. Shimizu *et al.*, Nature (London) **393**, 767 (1998).
[2] I. Goncharenko, Phys. Rev. Lett. **94**, 205701 (2005).
[3] L. F. Lundegaard *et al.*, Nature (London) **443**, 201 (2006).
[4] H. Fujihisa *et al.*, Phys. Rev. Lett. **97**, 085503 (2006).
[5] G. Weck, S. Desgreniers, P. Loubeyre, and M. Mezouar, Phys. Rev. Lett. **102**, 255503 (2009).
[6] C. Barrett, L. Meyer, and J. Wasserman, J. Chem. Phys. **47**, 592 (1967).
[7] M. Nicol, K. R. Hirsch, and W. B. Holzapfel, Chem. Phys. Lett. **68**, 49 (1979).
[8] S. Serra, G. Chiarotti, S. Scandolo, and E. Tosatti, Phys. Rev. Lett. **80**, 5160 (1998).
[9] J. B. Neaton and N. W. Ashcroft, Phys. Rev. Lett. **88**, 205503 (2002).
[10] Y. M. Ma, A. R. Oganov, and C. W. Glass, Phys. Rev. B **76**, 064101 (2007).
[11] S. Desgreniers, Y. Vohra, and A. Ruoff, J. Phys. Chem. **94**, 1117 (1990).
[12] Y. Akahama *et al.*, Phys. Rev. Lett. **74**, 4690 (1995).
[13] D. Y. Kim *et al.*, Phys. Rev. B **77**, 092104 (2008).
[14] J. S. Tse *et al.*, Solid State Commun. **145**, 5 (2008).
[15] M. I. Eremets *et al.*, Nature Mater. **3**, 558 (2004).
[16] C. J. Pickard and R. J. Needs, Phys. Rev. Lett. **102**, 125702 (2009).
[17] Y. M. Ma *et al.*, Phys. Rev. Lett. **102**, 065501 (2009).
[18] M. J. Lipp, W. J. Evans, B. J. Baer, and C. S. Yoo, Nature Mater. **4**, 211 (2005).
[19] J. Sun, D. D. Klug, C. J. Pickard, and R. J. Needs, Phys. Rev. Lett. **106**, 145502 (2011).
[20] V. Iota *et al.*, Nature Mater. **6**, 34 (2006).
[21] J. Sun *et al.*, Proc. Natl. Acad. Sci. U.S.A. **106**, 6077 (2009).
[22] C. J. Pickard and R. J. Needs, Nature Phys. **3**, 473 (2007).
[23] J. M. McMahon and D. M. Ceperley, Phys. Rev. Lett. **106**, 165302 (2011).
[24] R. Jeanloz *et al.*, Proc. Natl. Acad. Sci. U.S.A. **104**, 9172 (2007).
[25] M. D. Knudson, M. P. Desjarlais, and D. H. Dolan, Science **322**, 1822 (2008).
[26] J. H. Eggert *et al.*, Nature Phys. **6**, 40 (2009).
[27] J. Hawreliak *et al.*, Astrophys. Space Sci. **307**, 285 (2007).
[28] D. K. Bradley *et al.*, Phys. Rev. Lett. **102**, 075503 (2009).

[29] J. Sun, D. D. Klug, and R. Martonak, J. Chem. Phys. **130**, 194512 (2009).
[30] C. J. Pickard and R. J. Needs, Nature Mater. **9**, 624 (2010).
[31] K. D. Litasov, A. F. Goncharov, and R. J. Hemley, Earth Planet. Sci. Lett. **309**, 318 (2011).
[32] C. J. Pickard and R. J. Needs, Phys. Rev. Lett. **97**, 045504 (2006).
[33] C. J. Pickard and R. J. Needs, J. Phys. Condens. Matter **23**, 053201 (2011).
[34] J. P. Perdew, K. Burke, and M. Ernzerhof, Phys. Rev. Lett. **77**, 3865 (1996).
[35] S. J. Clark *et al.*, Z. Kristallogr. **220**, 567 (2005).
[36] G. Kresse and J. Furthmüller, Comput. Mater. Sci. **6**, 15 (1996).
[37] X. Gonze *et al.*, Comput. Mater. Sci. **25**, 478 (2002).
[38] See Supplemental Material at http://link.aps.org/supplemental/10.1103/PhysRevLett.108.045503 for more details of the methods, structures, phonon dispersion relations, and electronic bands.
[39] O. Degtyareva *et al.*, Nature Mater. **4**, 152 (2005).
[40] P. B. Allen and R. C. Dynes, Phys. Rev. B **12**, 905 (1975).